COMMUNICATION

Check for updates

Hybrid perovskite-like iodobismuthates as low-cost and stable anode materials for lithium-ion battery applications†

Kingshuk Roy,‡[ac] Tianyue Li,‡[b] Satishchandra Ogale [ID] *[ac] and Neil Robertson [ID] *[b]

We report the electrochemical applications of hybrid iodobismuthates [C$_3$H$_5$N$_2$]$_3$[Bi$_2$I$_9$] (IMB), [C$_2$H$_4$N$_3$S][BiI$_4$] (ADB) and [C$_3$H$_5$N$_2$S][BiI$_4$] (ATB), as a new type of environmentally-friendly anode for lithium-ion batteries. The materials show impressive Li-storage capacities along with very good rate capabilities and stability. The excellent properties of ATB, ADB and IMB indicate that further development and optimisation of this new family may be possible by further cation tuning within the series.§

Introduction

Due to ever increasing demand for robust, durable and cost effective stationary (grid) and transportable (laptops, mobile phones *etc.*) electrical energy storage, copious work has been done in the development of such energy storage devices. Among these, Li-ion batteries have achieved the best performance so far, with high stability, high energy density and low cost.[1–5] In addition, some more recent technologies in the energy storage field, such as Na-ion, Li–air, Na–air, Zn–air, Li–S *etc.* have also started to show growing promise.[6–19] These however, have yet to match the performance of Li-ion batteries and, in the current scenario, enormous studies are still essential in the field of Li-ion batteries to further increase stability, power and energy density, safety *etc.* Although carbon-based materials are the leading option in the case of insertion-based anode electrodes

[a]Department of Physics and Centre for Energy Science, Indian Institute of Science Education and Research, Pune, India. E-mail: satishogale@iiserpune.ac.in

[b]EaStCHEM School of Chemistry, University of Edinburgh, King's Buildings, David Brewster Road, Edinburgh EH93FJ, Scotland, UK. E-mail: neil.robertson@ed.ac.uk

[c]Research Institute for Sustainable Energy (RISE), TCG Centres for Research and Education in Science and Technology (TCG-CREST), BIPL Building, Salt Lake Sector V, Kolkata-700091, India

† Electronic supplementary information (ESI) available: Experimental synthesis and cell measurements; PXRD patterns; Impedance spectroscopy. See DOI: 10.1039/d0ta07414d

‡ These authors contributed equally to this work.

§ United Kingdom Patent Application No. 2008274.9.

in terms of cyclic stability and cost effectiveness, substantial research effort is going into developing different kinds of conversion, alloying and alloying-cum-conversion anodes due to the theoretical capacity limit (372 mA h g^{-1}) for graphitic carbons.[20–30] Although, alloying materials like Si, Sn, Ge, P *etc.* are of great interest due to their extremely high theoretical capacity (4200 mA h g^{-1} for Si, 992 mA h g^{-1} for Sn), they suffer from the inherent problem of huge volume expansion during lithiation and de-lithiation which limits their long-term stability and commercial use.[25,31–34] Many conversion and alloying-cum-conversion materials also suffer from the same issue. Hence, the utmost need to design an anode material capable of rendering a significantly higher capacity along with impressive stability. Recently, Zhong *et al.* have studied Bi nanoparticle anchored N-doped porous carbon as anodes for Li-ion batteries and achieved a reversible capacity of 300 mA h g^{-1} at a current density of 155 mA g^{-1}.[35] Also, Park *et al.* reported a Bi@C composite which showed a reversible capacity of 300 mA h g^{-1} after 100 cycles at 100 mA g^{-1} and Yang *et al.* reported Bi@C microspheres which showed a reversible capacity of 280 mA h g^{-1} after 100 cycles at 100 mA g^{-1}.[36,37] In addition, there are several reports on the oxides and sulfides of bismuth, however these also suffer the challenge of substantial volume expansion leading to poor stability.[38–42]

Hybrid lead–halide perovskites have emerged as the new generation of electronic materials for photovoltaic applications, optoelectronic devices, and energy storage devices. However, the adverse effects associated with the toxic element lead may limit practical application. Although there are reports where lead halide perovskites are being used as anode materials for Li-ion batteries, the stability of the material and toxicity of lead is still a drawback.[43–50] Bismuth, known as the least toxic heavy metal, is the most promising substitute for lead because of their similar electronic structures and properties. The inert 6s^2 electron pair is stereochemically inactive and thereby enables the formation of Bi–X (X = I, Br, Cl) octahedra as in lead–halide perovskites, and high structural tolerance of bismuth-based hybrid materials has been proven theoretically.[51] Bismuth–

This journal is © The Royal Society of Chemistry 2021

J. Mater. Chem. A, 2021, 9, 2689–2693 | 2689

halide perovskite-like materials have therefore attracted growing attention in their potential as photovoltaic, photodetector and supercapacitor materials, showing promising performance and enhanced stability.[52–56] However, we are unaware of any prior research carried out to study their potential as anode materials in lithium-ion batteries.

Herein, for the very first time we report Bi-based organic inorganic hybrid materials used as high-capacity and highly-stable anode materials for Li ion batteries. In this study, we have studied three different Bi based materials $[C_3H_5N_2]_3[Bi_2I_9]$ (IMB), $[C_2H_4N_3S][BiI_4]$ (ADB) and $[C_3H_5N_2S][BiI_4]$ (ATB). Alongside high capacity and stability it can be noted that Bi is a non-toxic material unlike the widely used Pb halide materials, which will avoid limitations associated with safety in manufacturing or use. Among the three hybrid materials used, IMB and ADB showed exceptional promise in terms of capacity values, although all the materials showed good lithiation de-lithiation stability. ADB, IMB and ATB showed a reversible capacity of 520 mA h g^{-1}, 450 mA h g^{-1} and 230 mA h g^{-1} respectively after 250 charging and discharging cycles. Furthermore, the materials have proven favourable in terms of power density by a very good rate performance when exposed to a variable current density.

Our study provides a preliminary and promising insight into low-cost and non-toxic iodobismuthate materials, and thereby establishes them as a new, tunable materials family for anode materials for lithium-ion batteries.

Schematic crystal structure diagrams of IMB, ADB and ATB are shown in Fig. 1, and full details of each structure can be found in the literature.[57,58] One-dimensional edge-sharing chains built by $[BiI_6]^{3-}$ octahedra can be found in both ATB and ADB, with organic counter-ions, 2-aminothiazolium and 2-amino-1,3,4-dithiazolium respectively, in between the chains. For IMB, zero-dimensional binuclear $[Bi_2I_9]^{3-}$ clusters construct the inorganic framework of the crystal structure, with highly disordered imidazolium as counter-ions. We aimed to exploit the inorganic skeleton of bismuth–iodides with lower dimensionality to better enable lithium ion insertion, via the one-dimensional Bi–I chains in ADB and ATB, and the zero-dimensional Bi–I binuclear octahedra in IMB. Fine powders of each material were prepared via fast precipitation directly from the solution of bismuth iodide with the counter-ion iodide salt. The powder diffraction patterns (PXRD) of the materials

(Fig. S1–S3†), showed a good match between the experimental PXRD peaks and those predicted from the published single-crystal structures. No indication of starting materials was shown in the diffraction patterns, indicating good product and phase purity.

The field-emission scanning electron microscopy (FESEM) images are provided in the ESI (Fig. S7–S9†). These show broadly-similar features for the three materials with crystallite sizes in the range around 100–200 nm.

Li-ion storage properties were measured for IMB, ADB and ATB. Coin cells with a lithium metal counter electrode were prepared using established methods. Constant current charge discharge data showed an initial discharge capacity of 1100 mA h g^{-1}, 930 mA h g^{-1}, and 1220 mA h g^{-1}, for IMB, ADB and ATB respectively, which includes solid electrolyte interphase (SEI) formation promoted by fluoroethylene carbonate additive, and subsequently reversible Li-ion capacity of 450 mA h g^{-1}, 520 mA h g^{-1}, and 230 mA h g^{-1} (Fig. 2a, 3a and 4a respectively) after 250 charge discharge cycle at an applied current density of 100 mA g^{-1}. Cyclic voltammetry measurements were also carried out to probe the mechanism of lithiation and de-lithiation, and in all three cases a reversible lithiation peak was found at ∼0.6 V. By analogy with literature, we assign this to the formation of Li$_3$Bi (Fig. 2b, 3b and 4b), although further experiments would be needed for this to be confirmed.[35] Also, in all the three cases, a reversible de-lithiation peak was found at ∼1 V.[35] A signature of reversible Li uptake can also be seen in the charge discharge curves (Fig. 2a, 3a and 4a). The lithiation voltage from charge discharge plots and from the cyclic voltammetry plots are clearly correlated (Fig. 2, 3 and 4 pink square). Further study will be required to probe whether the original material is reformed after cycling or if some structural changes occur.

Impressive rate performances were shown by IMB, ADB and ATB when exposed to current densities of 50 mA g^{-1}, 100 mA g^{-1}, 200 mA g^{-1}, 500 mA g^{-1}, 1 A g^{-1} and 2 A g^{-1}. Reversible capacities of 250 mA h g^{-1}, 200 mA h g^{-1} and 110 mA h g^{-1} were shown by IMB, ADB and ATB respectively
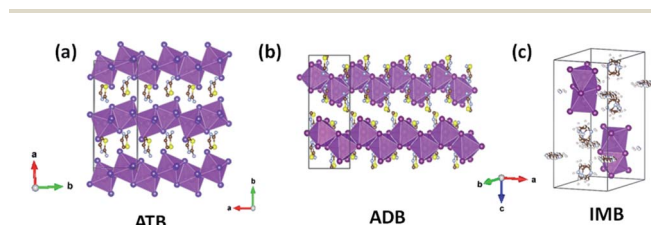

Fig. 1 Crystal structures for ATB (a), ADB (b) and IMB (c). Bismuth: magenta; iodine: purple; carbon: brown; sulfur: yellow; nitrogen: pale blue. The unit cell boundary is marked with dark lines, and bismuth iodide octahedra are shown in magenta. Hydrogen atoms are omitted for clarity.
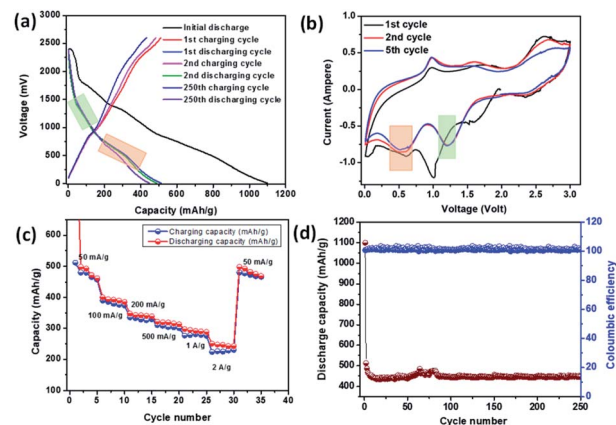

Fig. 2 Electrochemical performance of IMB anode in a coin cell with Li counter electrode (a) constant current charge−discharge (b) cyclic voltammetry (c) rate performance and (d) cycle stability.

2690 | J. Mater. Chem. A, 2021, 9, 2689–2693

This journal is © The Royal Society of Chemistry 2021

Fig. 3 Electrochemical performance of ADB anode in a coin cell with Li counter electrode (a) constant current charge–discharge (b) cyclic voltammetry (c) rate performance and (d) cycle stability.

Fig. 4 Electrochemical performance of ATB anode in a coin cell with Li counter electrode (a) constant current charge–discharge (b) cyclic voltammetry (c) rate performance and (d) cycle stability.
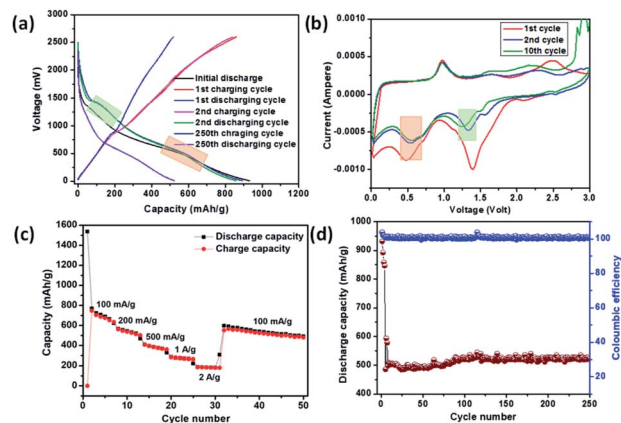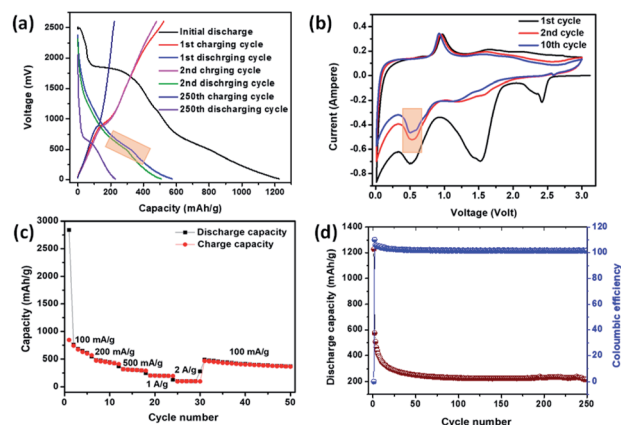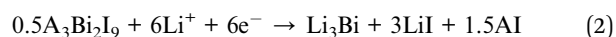
(Fig. 2c, 3c and 4c) when high current density of 2 A g^{-1} was employed. In all cases, the material showed excellent stability, with 100% retention of the reversible capacity after 250 charge discharge cycles (Fig. 2d, 3d and 4d). The electrochemical impedance spectra (EIS) analysis for the materials are also given in the ESI (Fig. S4–S6).† These data show a general correlation between series resistance and capacity, although further detailed studies are required to clarify the full mechanism. Tathavadekar *et al.* has shown a stable capacity of ~530 mA h g^{-1} after 250 cycles in a Pb containing 1D hybrid perovskite system. In terms of rate capabilities, they have shown current density of 0.5 A g^{-1} whereas, for our materials, especially for IMB, even at 2 A g^{-1} we could achieve a reversible capacity of more than 220 mA h g^{-1}.[45] Hence, both in terms of reversible capacity, cyclic stability and rate performance, we have shown excellent properties, comparable with Pb-containing hybrid perovskites. Moreover, Pb containing systems have severe problems of toxicity associated with these whereas, Bi is non-toxic.

The exceptionally high capacity of IMB and ADB is surprising, since formation of the Li$_3$Bi alloy from these materials can only lead to a theoretical capacity of 197, 196 and 182 mA h g^{-1} respectively, according to eqn (1) (ADB, ATB) and (2) (IMB). This limitation arises due to the high atomic masses of both bismuth and iodine. The anodes are hybrid materials however, comprising both organic and inorganic moieties. There are two major peaks involved during the reversible cathodic scan in the CV for all three compounds. The low potential peak at ~0.6 V is due to alloying to form Li$_x$Bi$_y$ which exist for all three anodes and is in good agreement with literature (*vide supra*). We note however, that for ADB and IMB, one extra lithiation peak is observed around 1.25–1.4 V, which is absent in the case of ATB (Fig. 2 and 3 green square). This process apparently provides the higher capacity of ADB and IMB compared with ATB. This is attributed to interaction of Li with the organic moiety, *e.g.* the –C≡N bond (for ADB) and the lone pair of nitrogen (for IMB) (Fig. S10†) which has precedence with the literature. However, the peak position and peak intensities vary for all three anodes and depend on reaction kinetics (diffusion and charge transfer). For example, lower peak intensities of ATB results in the lowest capacity and the highest charge transfer impedance among the three anodes. One of the possible explanations of the very low intensity of the peak corresponding to the interaction of Li with the organic –C≡N functional group in the case of ATB could be the lower π-electron density of the bond because of the ammonium cation such that the capacity value is less for this material compare to the other two systems.[50,51] The presence of more than one redox peak for each material may contribute to the somewhat sloping voltage profiles they show. Although further details on the origin of this process will require additional detailed mechanistic and structural studies including *in operando* measurements, beyond the scope of this initial communication. We also note that the voltage of around 500–1500 mV, although in the suitable range for anode application is not as ideal as *e.g.* graphite, typically around 100 mV.

$$ABiI_4 + 6Li^+ + 6e^- \rightarrow Li_3Bi + 3LiI + AI \qquad (1)$$

$$0.5A_3Bi_2I_9 + 6Li^+ + 6e^- \rightarrow Li_3Bi + 3LiI + 1.5AI \qquad (2)$$

Conclusions

We have shown, for the first time, Bi based organic–inorganic hybrid materials as candidates for reversible Li uptake and release when used as anode materials for Li-ion batteries. The systems not only showed a high Li storage property but also delivered an impressive power density when exposed to variable current density, and showed excellent stability over 250 cycles. The materials are environmentally friendly as a non-toxic material, Bi, was used. We believe that our work is highly novel and has the ability to open up a potentially-extensive and tuneable series of new compounds to be used as anodes for Li-ion batteries since the counterion can be further varied across a range of many other organic, and possibly inorganic, cations.

This journal is © The Royal Society of Chemistry 2021

J. Mater. Chem. A, 2021, **9**, 2689–2693 | **2691**

Conflicts of interest

There are no conflicts to declare.

Notes and references

1 M. Li, J. Lu, Z. Chen and K. Amine, *Adv. Mater.*, 2018, **30**, 1–24.

2 V. Etacheri, R. Marom, R. Elazari, G. Salitra and D. Aurbach, *Energy Environ. Sci.*, 2011, **4**, 3243–3262.

3 J. B. Goodenough and K. S. Park, *J. Am. Chem. Soc.*, 2013, **135**, 1167–1176.

4 J. Lu, Z. Chen, F. Pan, Y. Cui and K. Amine, *Electrochem. Energy Rev.*, 2018, **1**, 35–53.

5 P. Roy and S. K. Srivastava, *J. Mater. Chem. A*, 2015, **3**, 2454–2484.

6 L. Li, Y. Zheng, S. Zhang, J. Yang, Z. Shao and Z. Guo, *Energy Environ. Sci.*, 2018, **11**, 2310–2340.

7 N. Yabuuchi, K. Kubota, M. Dahbi and S. Komaba, *Chem. Rev.*, 2014, **114**, 11636–11682.

8 N. Imanishi and O. Yamamoto, *Mater. Today Adv.*, 2019, **4**, 100031.

9 N. Chawla and M. Safa, *Electronics*, 2019, **8**, 1201–1220.

10 V. Palomares, P. Serras, I. Villaluenga, K. B. Hueso, J. Carretero-González and T. Rojo, *Energy Environ. Sci.*, 2012, **5**, 5884–5901.

11 R. Kumar, J. Liu, J. Y. Hwang and Y. K. Sun, *J. Mater. Chem. A*, 2018, **6**, 11582–11605.

12 J. Christensen, P. Albertus, R. S. Sanchez-Carrera, T. Lohmann, B. Kozinsky, R. Liedtke, J. Ahmed and A. Kojic, *J. Electrochem. Soc.*, 2012, **159**.

13 K. N. Jung, J. Kim, Y. Yamauchi, M. S. Park, J. W. Lee and J. H. Kim, *J. Mater. Chem. A*, 2016, **4**, 14050–14068.

14 X. Xu, K. S. Hui, D. A. Dinh, K. N. Hui and H. Wang, *Mater. Horiz.*, 2019, 1306–1335.

15 S. K. Das, S. Lau and L. A. Archer, *J. Mater. Chem. A*, 2014, **2**, 12623–12629.

16 J. Fu, R. Liang, G. Liu, A. Yu, Z. Bai, L. Yang and Z. Chen, *Adv. Mater.*, 2018, **1805230**, 1–13.

17 Y. Li and H. Dai, *Chem. Soc. Rev.*, 2014, **43**, 5257–5275.

18 M. Barghamadi, A. Kapoor and C. Wen, *J. Electrochem. Soc.*, 2013, **160**, A1256–A1263.

19 A. Manthiram, Y. Fu, S. H. Chung, C. Zu and Y. S. Su, *Chem. Rev.*, 2014, **114**, 11751–11787.

20 K. Cao, T. Jin, L. Yang and L. Jiao, *Mater. Chem. Front.*, 2017, **1**, 2213–2242.

21 Y. Lu, L. Yu and X. W. Lou, *Chem*, 2018, **4**, 972–996.

22 H. H. Fan, H. H. Li, K. C. Huang, C. Y. Fan, X. Y. Zhang, X. L. Wu and J. P. Zhang, *ACS Appl. Mater. Interfaces*, 2017, **9**, 10708–10716.

23 M. N. Obrovac and V. L. Chevrier, *Chem. Rev.*, 2014, **114**, 11444–11502.

24 W. J. Zhang, *J. Power Sources*, 2011, **196**, 13–24.

25 K. Roy, M. Wahid, D. Puthusseri, A. Patrike, S. Muduli, R. Vaidhyanathan and S. Ogale, *Sustainable Energy Fuels*, 2019, **3**, 245–250.

26 F. Kong, L. Lv, Y. Gu, S. Tao, X. Jiang, B. Qian and L. Gao, *J. Mater. Sci.*, 2019, **54**, 4225–4235.

27 X. Ma, L. Zou and W. Zhao, *Chem. Commun.*, 2018, **54**, 10507–10510.

28 J. M. Yan, H. Z. Huang, J. Zhang, Z. J. Liu and Y. Yang, *J. Power Sources*, 2005, **146**, 264–269.

29 Y. P. Wu, E. Rahm and R. Holze, *J. Power Sources*, 2003, **114**, 228–236.

30 L. S. Roselin, R. Juang, C. Hsieh, S. Sagadevan, A. Umar, R. Selvin and H. H. Hegazy, *Materials*, 2019, **12**, 1229.

31 M. Ashuri, Q. He and L. L. Shaw, *Nanoscale*, 2016, **8**, 74–103.

32 P. Li, G. Zhao, X. Zheng, X. Xu, C. Yao, W. Sun and S. X. Dou, *Energy Storage Mater.*, 2018, **15**, 422–446.

33 M. G. Park, D. H. Lee, H. Jung, J. H. Choi and C. M. Park, *ACS Nano*, 2018, **12**, 2955–2967.

34 H. Ying and W. Q. Han, *Adv. Sci.*, 2017, **4**, 1700298.

35 Y. Zhong, B. Li, S. Li, S. Xu, Z. Pan, Q. Huang, L. Xing, C. Wang, W. Li and C. Wang, *Nano-Micro Lett.*, 2018, **10**, 1–14.

36 C. M. Park, S. Yoon, S. Il Lee and H. J. Sohn, *J. Power Sources*, 2009, **186**, 206–210.

37 F. Yang, F. Yu, Z. Zhang, K. Zhang, Y. Lai and J. Li, *Chem.–Eur. J.*, 2016, **22**, 2333–2338.

38 Y. Dong, M. Hu, Z. Zhang, J. A. Zapien, X. Wang and J. M. Lee, *Nanoscale*, 2018, **10**, 13343–13350.

39 W. Chai, F. Yang, W. Yin, S. You, K. Wang, W. Ye, Y. Rui and B. Tang, *Dalton Trans.*, 2019, **48**, 1906–1914.

40 Z. Deng, T. Liu, T. Chen, J. Jiang, W. Yang, J. Guo, J. Zhao, H. Wang and L. Gao, *ACS Appl. Mater. Interfaces*, 2017, **9**, 12469–12477.

41 Y. Li, M. A. Trujillo, E. Fu, B. Patterson, L. Fei, Y. Xu, S. Deng, S. Smirnov and H. Luo, *J. Mater. Chem. A*, 2013, **1**, 12123–12127.

42 S. Liu, Z. Cai, J. Zhou, A. Pan and S. Liang, *J. Alloys Compd.*, 2017, **715**, 432–437.

43 N. Vicente and G. Garcia-Belmonte, *J. Phys. Chem. Lett.*, 2017, **8**, 1371–1374.

44 H. R. Xia, W. T. Sun and L. M. Peng, *Chem. Commun.*, 2015, **51**, 13787–13790.

45 M. Tathavadekar, S. Krishnamurthy, A. Banerjee, S. Nagane, Y. Gawli, A. Suryawanshi, S. Bhat, D. Puthusseri, A. D. Mohite and S. Ogale, *J. Mater. Chem. A*, 2017, **5**, 18634–18642.

46 Q. Wang, T. Yang, H. Wang, J. Zhang, X. Guo, Z. Yang, S. Lu and W. Qin, *CrystEngComm*, 2019, **21**, 1048–1059.

47 A. Kostopoulou, D. Vernardou, K. Savva and E. Stratakis, *Nanoscale*, 2019, **11**, 882–889.

48 W. Zhang, G. E. Eperon and H. J. Snaith, *Nat. Energy*, 2016, **1**, 16048.

49 H. R. Xia, W. T. Sun and L. M. Peng, *Chem. Commun.*, 2015, **51**, 13787–13790.

50 N. Vicente and G. Garcia-Belmonte, *J. Phys. Chem. Lett.*, 2017, **8**, 1371–1374.

51 R. A. Wheeler and P. N. V. P. Kumar, *J. Am. Chem. Soc.*, 1992, **114**, 4776–4784.

52 L. Zhang, K. Wang and B. Zou, *ChemSusChem*, 2019, **12**, 1612–1630.

2692 | *J. Mater. Chem. A*, 2021, **9**, 2689–2693

This journal is © The Royal Society of Chemistry 2021

53 N. C. Miller and M. Bernechea, *APL Mater.*, 2018, **16**, 084503.

54 Z. Qi, X. Fu, T. Yang, D. Li, P. Fan, H. Li, F. Jiang, L. Li, Z. Luo, X. Zhuang and A. Pan, *Nano Res.*, 2019, **12**, 1894–1899.

55 K. Adams, A. F. González, J. Mallows, T. Li, J. H. J. Thijssen and N. Robertson, *J. Mater. Chem. A*, 2019, **7**, 1638–1646.

56 T. Li, J. Mallows, K. Adams, G. S. Nichol, J. H. J. Thijssen and N. Robertson, *Batteries Supercaps*, 2019, **2**, 568–575.

57 T. Li, Q. Wang, G. S. Nichol, C. A. Morrison, H. Han, Y. Hu and N. Robertson, *Dalton Trans.*, 2018, **47**, 7050–7058.

58 V. G. Campi, *J. Chem. Crystallogr.*, 1994, **24**, 3–6.

This journal is © The Royal Society of Chemistry 2021

J. Mater. Chem. A, 2021, **9**, 2689–2693 | **2693**